JOURNAL OF GUIDANCE, CONTROL, AND DYNAMICS
Vol. 32, No. 1, January–February 2009

Engineering Notes

ENGINEERING NOTES are short manuscripts describing new developments or important results of a preliminary nature. These Notes should not exceed 2500 words (where a figure or table counts as 200 words). Following informal review by the Editors, they may be published within a few months of the date of receipt. Style requirements are the same as for regular contributions (see inside back cover).

State-Dependent Riccati-Equation-Based Guidance Law for Impact-Angle-Constrained Trajectories

Ashwini Ratnoo* and Debasish Ghose†
Indian Institute of Science, Bangalore, 560 012, India

DOI: 10.2514/1.37876

I. Introduction

IN MANY advanced guidance applications, it is required to intercept the target from a particular direction: that is, to achieve a certain impact angle [1–3]. Closed-form solutions for energy-optimal impact-angle-constrained guidance laws have been proposed for a stationary target by Ryoo et al. [4], who used the linear quadratic regulator technique after linearizing the engagement kinematics. The guidance law proposed by them captures all impact angles from any initial launch angle in a planar engagement scenario. Lu et al. [5] solved the problem of guiding a hypersonic gliding vehicle in its terminal phase to a stationary target using adaptive proportional navigation guidance. Ohlmeyer and Phillips [6] extended the idea of explicit guidance (proposed by Cherry [7]) to include a terminal impact angle constraint. However, the simulations by Ohlmeyer and Phillips [6] are carried out only for a vertical impact against a stationary target, and the impact angle errors encountered are sensitive to the launch altitude.

A promising technique for designing nonlinear controllers for nonlinear systems is the state-dependent Riccati equation (SDRE) [8,9] approach. In its classical formulation, this extended linearization method uses a state-dependent coefficient (SDC) parameterization of the nonlinear system, together with a nonlinear performance index with quadraticlike structure, to reduce the control problem to the solution of a state-dependent Riccati equation.

As the main contribution of this Note, we solve the impact-angle-constrained guidance problem against a stationary target as a nonlinear regulator problem using the SDRE technique. The problem is solved using a time-varying state weighting matrix Q, which is assumed to be a function of time-to-go and controls the states, depending on the relative target position. A constant-speed missile model is assumed for deriving the guidance law. Numerical simulations for a realistic missile model are carried out with given vehicle model and aerodynamic properties. Simulations are carried out for different impact angles and initial firing angles. Robustness of the proposed guidance law with respect to autopilot lag is verified by simulations.

Presented as Paper 6539 at the AIAA Guidance Navigation, and Control Conference and Exhibit, Hilton Head, SC, 20–23 August 2007; received 3 April 2008; revision received 11 July 2008; accepted for publication 16 September 2008.

*Graduate Student, Department of Aerospace Engineering; jmk@aero.iisc.ernet.in.

†Professor, Department of Aerospace Engineering; dghose@aero.iisc.ernet.in.

II. Guidance Problem and The SDRE Solution

Consider a planar engagement scenario, as shown in Fig. 1. We consider a lag-free constant-speed missile model and a stationary target. The two missile states are the cross-range z and the heading angle θ_m. We assume ideal sensor information during the engagement. The nonlinear system dynamics is represented by Eqs. (1) and (2):

$$\dot{z} = v_m \sin\theta_m \tag{1}$$

$$\dot{\theta}_m = a_m / v_m \tag{2}$$

where a_m is the control or the missile lateral acceleration applied normal to the missile heading direction. Here, the objective is to hit the target at zero impact angle: that is, $\theta_{mf} = 0$ deg. Thus, the guidance problem can be formulated as a nonlinear regulator problem in which both states z and θ_m go to zero as the interceptor approaches the target.

A. Cost Function and SDC Parametrization

We have the two states as

$$\mathbf{x} = \begin{bmatrix} z \\ \theta_m \end{bmatrix} \tag{3}$$

The SDC form of the equations is given as

$$\dot{\mathbf{x}} = \mathbf{A}(\mathbf{x})\mathbf{x} + \mathbf{B}u \tag{4}$$

Putting Eqs. (1) and (2) in the SDC form,

$$\dot{z} = v_m \left(\frac{\sin\theta_m}{\theta_m}\right)\theta_m \tag{5}$$

$$\dot{\theta}_m = \frac{a_m}{v_m} \tag{6}$$

From Eqs. (3–6), we get

$$\mathbf{A}(\mathbf{x}) = \begin{bmatrix} 0 & \frac{v_m \sin\theta_m}{\theta_m} \\ 0 & 0 \end{bmatrix} \tag{7}$$

$$\mathbf{B} = \begin{bmatrix} 0 \\ \frac{1}{v_m} \end{bmatrix} \tag{8}$$

Consider a general infinite-horizon nonlinear regulator problem in which we minimize

$$J = \frac{1}{2}\int_{t_0}^{\infty} [\mathbf{x}^T \mathbf{Q}\mathbf{x} + Ru^2(t)]\mathrm{d}t \tag{9}$$

with respect to $\mathbf{x}$ and u subject to Eq. (4). Here, $\mathbf{Q}$ and R are the state weighting matrix and the control weighting matrix, respectively.

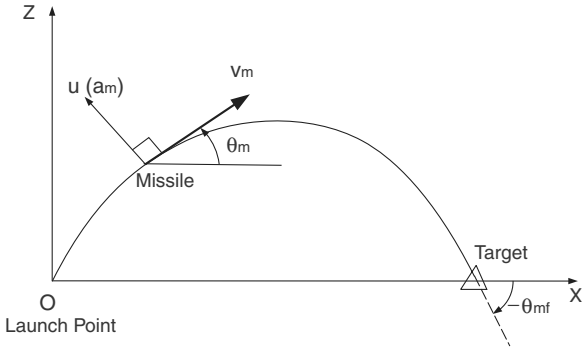

Fig. 1 Engagement geometry.

Also, $\mathbf{Q}$ and R are the two design parameters available to us for obtaining the desired control. We assume

$$R = 1 \tag{10}$$

and $\mathbf{Q}$ to be some function of t_{go} to include the target information in the guidance logic:

$$\mathbf{Q} = \begin{bmatrix} q_1^2 & 0 \\ 0 & q_2^2 \end{bmatrix} \tag{11}$$

We check the conditions for the SDRE control solution to be locally asymptotically stable as given in [8,9].

1) The pair $\{\mathbf{A}(\mathbf{x}), \mathbf{B}\}$ should be controllable in the domain of interest. Using Eqs. (7) and (8), we have

$$|\{\mathbf{B}, \mathbf{A}(\mathbf{x})\mathbf{B}\}| = -\frac{\sin\theta_m}{v_m\theta_m} \neq 0 \tag{12}$$

for all values of θ_m except at $\theta_m = \pi$. We consider $\theta_m = \pi$ to be outside the domain of interest.

2) The function $f(\mathbf{x}) = \mathbf{A}(\mathbf{x})\mathbf{x} \in C^1$. Using Eqs. (3) and (7),

$$\mathbf{A}(\mathbf{x})\mathbf{x} = \begin{bmatrix} v_m \sin\theta_m \\ 0 \end{bmatrix} \in C^1 \tag{13}$$

3) The initial condition $f(0) = 0$. Using Eq. (13),

$$f(0) = \begin{bmatrix} v_m \sin 0 \\ 0 \end{bmatrix} = \begin{bmatrix} 0 \\ 0 \end{bmatrix} \tag{14}$$

4) The matrix $\mathbf{B}(\mathbf{x}) \neq \mathbf{0}$. From Eq. (8) we have $\mathbf{B}$ as a constant nonzero matrix.

5) The matrix $\mathbf{Q} \geq 0$ and $R > 0$. From Eqs. (10) and (11), these conditions are met.

B. Solving SDRE

We solve for $\mathbf{P}$ (≥ 0) using the algebraic state-dependent Riccati equation as

$$\mathbf{A}^T(\mathbf{x})\mathbf{P}(\mathbf{x}) + \mathbf{P}(\mathbf{x})\mathbf{A}(\mathbf{x}) - \mathbf{P}(\mathbf{x})\mathbf{B}\mathbf{R}^{-1}\mathbf{B}^T\mathbf{P}(\mathbf{x}) + \mathbf{Q} = 0 \tag{15}$$

where

$$\mathbf{P}(\mathbf{x}) = \begin{bmatrix} p_{11} & p_{12} \\ p_{12} & p_{22} \end{bmatrix} \tag{16}$$

Using Eqs. (7), (8), (10), (11), and (16) in Eq. (15), we have

$$\begin{bmatrix} 0 & 0 \\ \frac{v_m \sin(\theta_m)}{\theta_m} & 0 \end{bmatrix}\begin{bmatrix} p_{11} & p_{12} \\ p_{12} & p_{22} \end{bmatrix} + \begin{bmatrix} p_{11} & p_{12} \\ p_{12} & p_{22} \end{bmatrix}\begin{bmatrix} 0 & \frac{v_m \sin(\theta_m)}{\theta_m} \\ 0 & 0 \end{bmatrix} - \begin{bmatrix} p_{11} & p_{12} \\ p_{12} & p_{22} \end{bmatrix}\begin{bmatrix} 0 \\ \frac{1}{v_m} \end{bmatrix}\begin{bmatrix} 0 & \frac{1}{v_m} \end{bmatrix}\begin{bmatrix} p_{11} & p_{12} \\ p_{12} & p_{22} \end{bmatrix} + \begin{bmatrix} q_1^2 & 0 \\ 0 & q_2^2 \end{bmatrix} = 0 \tag{17}$$

Solving, we have

$$p_{11} = q_1 \frac{\theta_m}{v_m \sin\theta_m}\sqrt{q_2^2 + 2q_1 v_m^2 \frac{\sin\theta_m}{\theta_m}} \tag{18}$$

$$p_{12} = q_1 v_m \tag{19}$$

$$p_{22} = v_m \sqrt{q_2^2 + 2q_1 v_m^2 \frac{\sin\theta_m}{\theta_m}} \tag{20}$$

C. Nonlinear Feedback Control

The SDRE control is given by

$$u^* = -\mathbf{B}^T\mathbf{P}(\mathbf{x})\mathbf{x} \tag{21}$$

Using Eqs. (16) and (18–20) in Eq. (21),

$$u^* = -\left(q_1 z + \sqrt{q_2^2 + 2q_1 v_m^2 \frac{\sin\theta_m}{\theta_m}}\theta_m\right) \tag{22}$$

because we are interested only in the terminal value of θ_m and not its intermediate values, we choose

$$q_2 = 0 \tag{23}$$

The cross-range position z should be controlled tightly for successful interception. Therefore, we choose q_1 to be a function of time-to-go as

$$q_1 = \left(\frac{N}{t_{\text{go}}}\right)^2 \tag{24}$$

where N is a positive constant. Using Eqs. (23) and (24) in Eq. (22), we get the control command as

$$u^* = -\left\{\left(\frac{N}{t_{\text{go}}}\right)^2 z + \frac{\sqrt{2}Nv_m}{t_{\text{go}}}\sqrt{\frac{\sin\theta_m}{\theta_m}}\theta_m\right\} \tag{25}$$

which can be compared with proportional-navigation-based guidance laws. Note that although $q_2 = 0$, the nonlinear regulator command [see Eq. (25)] still has a nonzero coefficient for the second state θ_m, thus also regulating the second state to zero at the time of interception. Setting q_2 to zero eliminates additional running cost on the second state [see Eq. (22)], thus reducing the control requirement and resulting in a simple guidance law of a form similar to that of the proportional navigation.

The cross-range value z can be computed using the line-of-sight separation R and line-of-sight angle θ as (see Fig. 2)

$$z = R\sin(-\theta) \tag{26}$$

Using Eqs. (25) and (26), we obtain the SDRE nonlinear regulator guidance command as

$$u^* = -\left\{\left(\frac{N}{t_{\text{go}}}\right)^2 R\sin(-\theta) + \frac{\sqrt{2}Nv_m}{t_{\text{go}}}\sqrt{\frac{\sin\theta_m}{\theta_m}}\theta_m\right\} \tag{27}$$

Time-to-go is computed as

$$t_{\text{go}} = \frac{R}{v_{\text{ref}}} \tag{28}$$

where v_{ref} is the reference velocity for evaluating time-to-go. Closing velocity V_c is taken to be the reference velocity as long as it is greater than $v_m/2$. Because of high heading errors, some engagements may have zero or even negative closing velocity for the initial phase of the

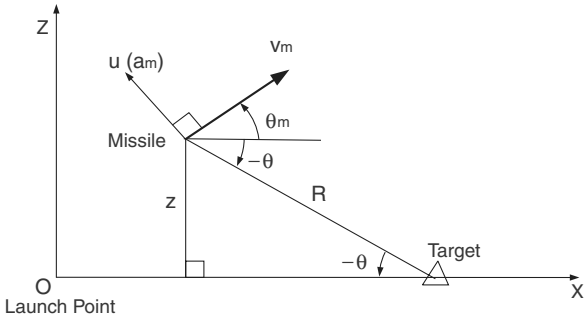

Fig. 2 Line-of-sight parameters.

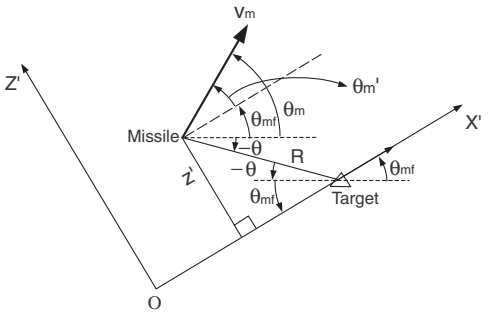

Fig. 3 Generalized impact geometry.

engagement, thus resulting in a poor time-to-go estimate. Therefore, we use the following logic for evaluating the reference velocity:

$$v_{\text{ref}} = \begin{cases} V_c & \text{if } V_c > v_m/2 \\ v_m/2 & \text{if } V_c \le v_m/2 \end{cases} \tag{29}$$

Under high-heading-error conditions, we assume $v_m/2$ as the average closing velocity.

III. Extension to Arbitrary Impact Angles

The guidance command given by Eq. (27) is a regulator solution resulting in zero impact angle. Consider the engagement geometry for an arbitrary impact angle as shown in Fig. 3. The desired impact angle is θ_{mf}. We consider a new frame of reference $X'OZ'$ with its X axis along the desired impact angle. The guidance problem now becomes a regulator problem in the new frame of reference. The missile cross-range z' and heading θ'_m values in the new frame of reference are computed as

$$z' = R\sin(\theta_{mf} - \theta) \tag{30}$$

$$\theta'_m = (\theta_m - \theta_{mf}) \tag{31}$$

Using Eqs. (30) and (31) in Eq. (25), we have

$$u^* = -\left\{\left(\frac{N}{t_{\text{go}}}\right)^2 R\sin(\theta_{mf} - \theta) + \frac{\sqrt{2}Nv_m}{t_{\text{go}}}\sqrt{\frac{\sin(\theta_m - \theta_{mf})}{(\theta_m - \theta_{mf})}}(\theta_m - \theta_{mf})\right\} + g\cos\theta_m \tag{32}$$

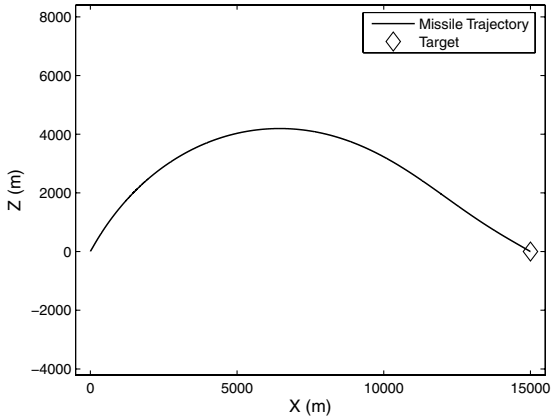

a) Missile trajectory

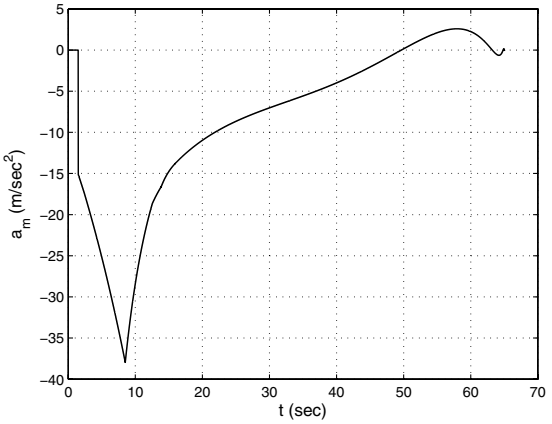

b) Control (lateral acceleration)

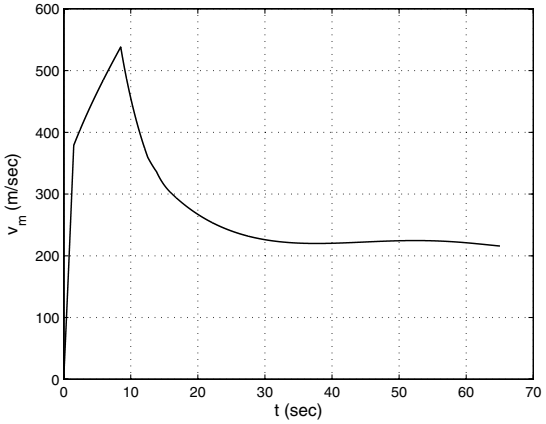

c) Missile speed

Fig. 4 Results of case 1: a typical engagement.

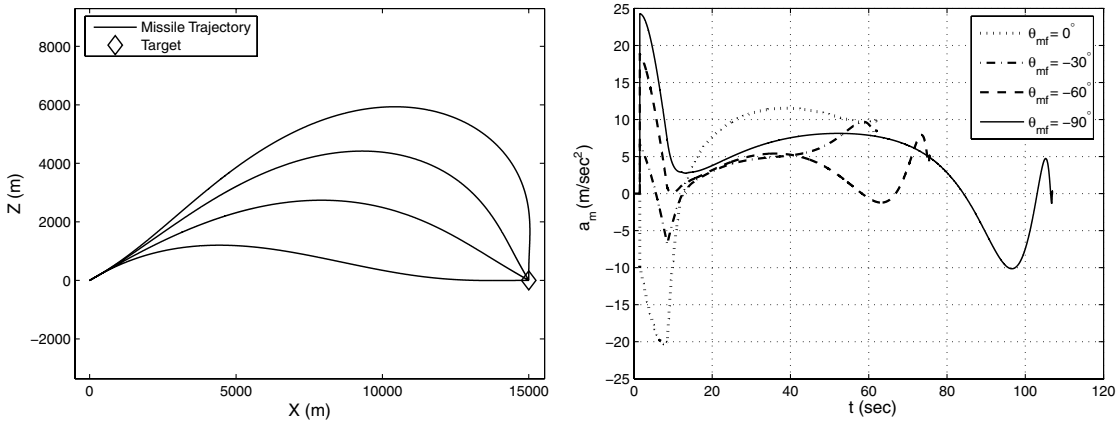

a) Missile trajectories **b) Lateral acceleration profiles**

Fig. 5 Results of case 2: different impact angles.

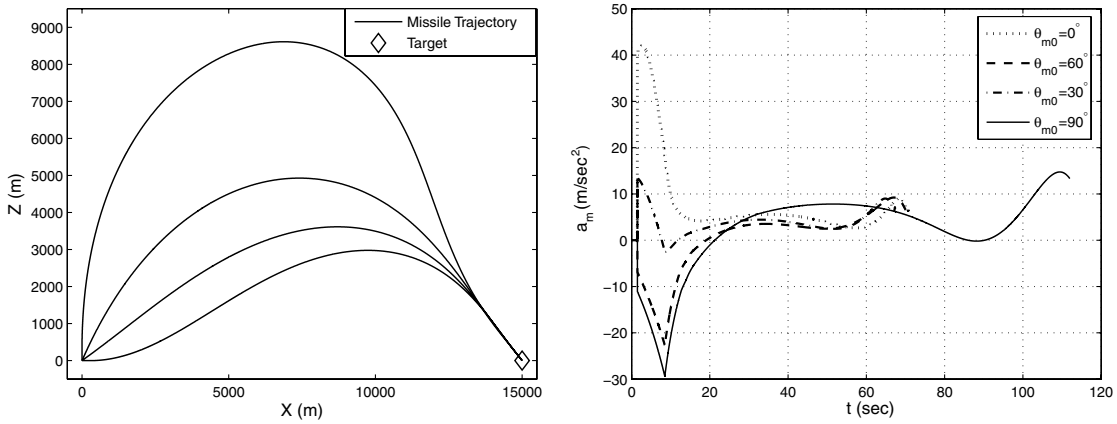

a) Missile trajectories **b) Lateral acceleration profiles**

Fig. 6 Results of case 3: different launch angles.

The last term in Eq. (32) is added for gravity compensation in a vertical plane engagement scenario.

IV. Simulation Results

The guidance law derived in Eq. (32) assumes the constant-speed kinematic missile model given by Eqs. (1) and (2). For simulations, we use a realistic missile model as a point mass flying over a flat, nonrotating, Earth. The detailed model with aerodynamic and vehicle properties is borrowed from Kee et al. [10]. In all the simulations, the maximum lateral acceleration limit for the missile is taken to be $\pm 15\ g$. The simulations, unless specified, are carried out with $(x_m, z_m) = (0, 0)$, $(x_t, z_t) = (15\text{ km}, 0)$, and $N = 3$ and are terminated at a closing distance of less than 0.1 m. The corresponding impact angle errors are less than 10^{-3} deg.

A. Case 1: A Typical Surface-to-Surface Engagement

As a typical surface-to-surface engagement, we consider the missile firing angle $\theta_{m0} = 60$ deg and the desired impact angle $\theta_{mf} = -30$ deg. The missile trajectory is plotted in Fig. 4a. The corresponding control history (after subtracting the gravity compensation component) is shown in Fig. 4b. Results show successful interception of the target with the desired impact angle. The control command goes to zero at interception, which is a desirable characteristic. The missile speed vs time is plotted in Fig. 4c.

B. Case 2: Different Impact Angles with the Same Initial Geometry

Here, we simulate trajectories for different impact angles $\theta_{mf} = 0$, -30, -60, and -90 deg, with the same launch angle $\theta_{m0} = 30$ deg. The missile trajectories are plotted in Fig. 4a. The corresponding control histories are plotted in Fig. 5b. Trajectories with higher average curvature have higher terminal lateral acceleration demand. Results show the capability of the proposed guidance law to hit the target at different impact angles, depending on the mission requirement.

C. Case 3: Different Launch Angles with the Same Impact Angle Requirement

Here, we simulate trajectories with different launch angles $\theta_{m0} = 0, 30, 60$, and 90 deg and a fixed impact angle $\theta_{mf} = -45$ deg. The trajectories and control histories are plotted in Figs. 6a and 6b, respectively. Simulations show the capability of the proposed guidance law to hit the target at a given impact angle with different launch angles.

D. Case 4: Effect of N on the Performance

So far, we have assumed the state weighting matrix gain $N = 3$. Here, we investigate the effect of the choice of N on the engagement. We choose $N \in [2, 4]$ with $\theta_{m0} = 70$ deg and $\theta_{mf} = -30$ deg for the simulations. For $N = 2, 3$, and 4, the trajectories and control histories are shown in Figs. 7a and 7b. With higher values of N ($N = 4$ in

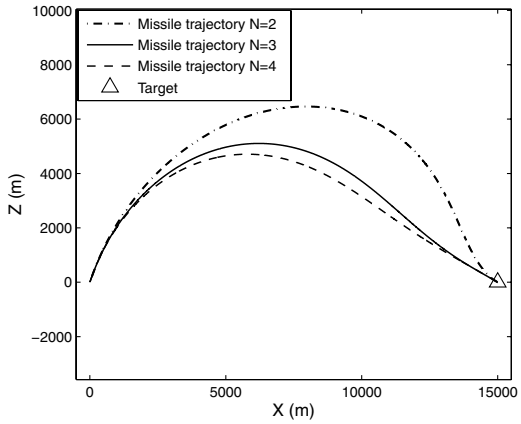

a) Missile trajectory

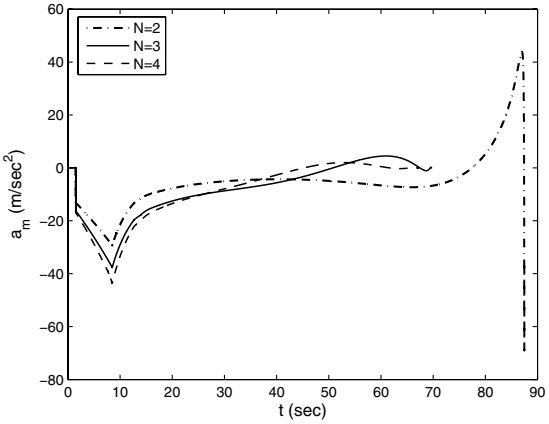

b) Lateral acceleration profiles

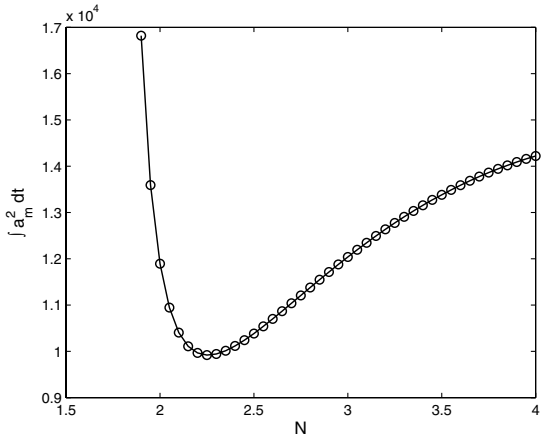

c) Integral control effort vs N

Fig. 7 Results of case 4: effect of N on the performance.

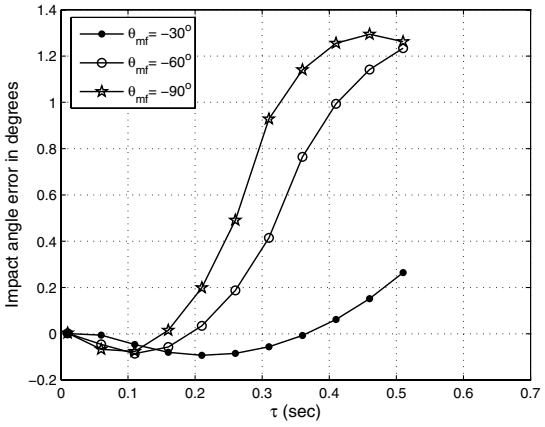

a) Impact angle error vs τ

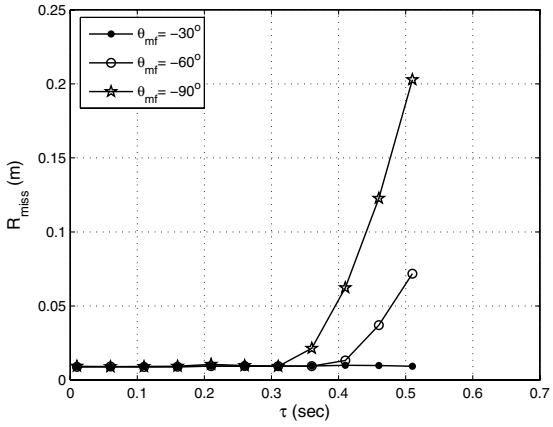

b) Miss distance vs τ

Fig. 8 Results of case 5: studies with system lag.

Fig. 7b), the lateral acceleration demand is higher initially and reduces near interception. We compute the integral control effort corresponding to the different values of N as

$$CE = \int_{t_0}^{t_f} a_m^2 \mathrm{d}t \tag{33}$$

The result is plotted in Fig. 7c. Numerical results show that there exists a minimum value of the total control effort with respect to N. The simulations highlight the capability of SDRE design as a control shaping technique. Constraints of the maximum actuator rates and saturation can thus be made compatible with the guidance command by suitable choice of the weight N. Finally, the weight can be decided based on the total control effort and control shape required.

E. Case 5: Robustness with Respect to System Lag

Here, we test the robustness of the proposed guidance law with respect to the missile system delays. No compensation is incorporated for the delays in the guidance logic. The overall missile delays are modeled as first-order delay as

$$\frac{a_m}{u} = \frac{1}{s\tau + 1} \tag{34}$$

where τ is the first-order time constant. Simulations are carried out with $\theta_{m0} = 30\,\text{deg}$ and $\theta_{mf} = -30$, -60, and $-90\,\text{deg}$.

The impact angle errors and the miss distance for different values of τ are plotted in Figs. 8a and 8b. We see that the errors are very low for uncompensated first-order delays up to 0.5 s. The results also show that robustness performance depends on the impact angle. Higher errors are encountered for trajectories with high average curvature. The results prove the robustness of the proposed guidance law with respect to system delays.

V. Conclusions

The impact-angle-constrained guidance problem is solved as a nonlinear regulator problem using the state-dependent Riccati equation (SDRE) technique. A planar engagement scenario is considered with a stationary target. The state weighting matrix is chosen as a function of time-to-go for the design. The resulting regulator control is extended to a general impact angle by rotating the frame of reference along the desired impact angle. The performance of the proposed guidance law is tested numerically for a realistic missile model. Simulations are carried out for different impact angles and initial firing conditions. Results show negligible errors for miss distance and the desired impact angle. The SDRE design also highlights the freedom for shaping the control history. Robustness studies with uncompensated first-order missile delays up to 0.5 s show very low errors in impact angle and miss distance.

References

[1] Kim, M., and Grider, K. V., "Terminal Guidance for Impact Attitude Angle Constrained Flight Trajectories," *IEEE Transactions on Aerospace and Electronic Systems*, Vol. AES-9, Dec. 1973, pp. 852–859.
doi:10.1109/TAES.1973.309659

[2] York, R. J., and Pastrick, H. L., "Optimal Terminal Guidance with Constraints at Final Time," *Journal of Spacecraft and Rockets*, Vol. 14, June 1977, pp. 381–382.
doi:10.2514/3.57212

[3] Kim, B. S., Lee, J. G., and Han, H. S., "Biased PNG Law for Impact with Angular Constraint," *IEEE Transactions on Aerospace and Electronic Systems*, Vol. AES-34, Jan. 1998, 277–288.

[4] Ryoo, C. K., Cho, H., and Tahk, M. J., "Optimal Guidance Laws with Terminal Impact Angle Constraint," *Journal of Guidance, Control, and Dynamics*, Vol. 28, No. 4, July–August 2005, pp. 724–732.
doi:10.2514/1.8392

[5] Lu, P., Doman, D. B., and Schierman, J. D., "Adaptive Terminal Guidance for Hypervelocity Impact in Specified Direction," *Journal of Guidance, Control, and Dynamics*, Vol. 29, No. 2, Mar.–Apr. 2006, pp. 269–278.
doi:10.2514/1.14367

[6] Ohlmeyer, E. J., and Phillips, C. A., "Generalized Vector Explicit Guidance," *Journal of Guidance, Control, and Dynamics*, Vol. 29, No. 2, Mar.–Apr. 2006, pp. 261–268.
doi:10.2514/1.14956

[7] Cherry, G., "A General Explicit, Optimizing Guidance Law for Rocket-Propelled Spacecraft," *AIAA Astrodynamics, Guidance and Control Conference*, AIAA Paper 64-638, August 1964.

[8] Cloutier, J. R., "State-Dependent Riccati Equation Techniques: An Overview," *Proceedings of the American Control Conference*, Inst. of Electrical and Electronics Engineers, Piscataway, NJ, June 1997, pp. 932–936.

[9] Cloutier, J. R., and Stansbery, D. T., "The Capabilities and Art of State-Dependent Riccati Equation-Based Design," *Proceedings of the American Control Conference* Anchorage, AK, Inst. of Electrical and Electronics Engineers, Piscataway, NJ, May 2002, pp. 86–91.

[10] Kee, P. E., Dong, L., and Siong, C. J., "Near Optimal Midcourse Guidance Law for Flight Vehicle," 36th AIAA Aerospace Sciences Meeting and Exhibit, Reno, NV, AIAA Paper 98-0583, Jan. 1998.